Generation of quadripartite unlockable bound entanglement from cascaded four-wave mixing processes

Jun Xin,[1,*] Xiao-Ming Lu,[1] Guolong Li,[1] and Jietai Jing[2,3,4]

[1]*Department of Physics, Hangzhou Dianzi University, Hangzhou* 310018*, China*

[2]*State Key Laboratory of Precision Spectroscopy, School of Physics and Materials Science, East China Normal University, Shanghai* 200062*, People's Republic of China*

[3]*Collaborative Innovation Center of Extreme Optics, Shanxi University, Taiyuan, Shanxi 030006, People's Republic of China*

[4]*Department of Physics, Zhejiang University, Hangzhou* 310027*, China*

(Received 30 January 2019; published 28 May 2019)

We propose a scheme for generating a continuous-variable (CV) quadripartite unlockable bound entangled state from cascaded four-wave mixing processes. Different from the previous method involving a bipartite entangled state and two thermal states, our results show that the CV quadripartite unlockable bound entangled state can be generated via the internal reconfiguration of a four-mode entangled state. Both the nondistillability and superactivation of the generated CV quadripartite unlockable bound entangled state can be demonstrated. We believe that our scheme is experimentally accessible and will contribute to a deeper understanding of CV multipartite unlockable bound entanglement.

DOI: 10.1103/PhysRevA.99.053840

I. INTRODUCTION

Quantum entangled resources [1], which play a central role in quantum physics, utilize the unique properties of the quantum systems to fulfill computing, communication, and measurement tasks, and own advantages over the classical systems. In a realistic setting, a quantum entangled state is very fragile and can be easily degraded to be mixed by the unwanted decoherence processes from the environment. For a wide class of mixed entangled states, it has been shown that they can be distilled to become maximally entangled states by means of the distillation protocol [2,3]. Therefore, such mixed entangled states can be used as available resources in quantum communication and quantum computation. However, there exists a set of so-called bound entangled states [4] from which no pure entanglement can be distilled. Despite the nondistillability of the bound entangled state, two sets of multipartite bound entangled states tensored together can make a distillable state, which is known as "superactivation" (or "unlockability"). For superactivation, two sets of multipartite bound entangled states ρ_1, ρ_2 are combined to yield more pure entanglement than the sum of what a set of parties could distill from either ρ_1 or ρ_2 on their own, even if many copies of ρ_1 or ρ_2 are shared [5]. Experimentally, the superactivation can be realized by dividing all the parties of ρ_1, ρ_2 into several groups and making some of the groups joined together by performing collective quantum operations. Then pure entanglement may be distilled from the two parties within some of the divided groups [5,6]. In the last two decades, bound entanglement has attracted considerable attention. Much effort has been devoted to the underlying physical properties of the bound entanglement such as its relationship with the positive partial transpose condition [4,7–9], the stabilizer formalism [10,11], and the Bell inequalities [12–14]. Moreover, it has been found that the bound entanglement has its practical implications in quantum cryptography [15–19], quantum teleportation [20,21], quantum metrology [22], remote information concentration [23], and reducing communication complexity [24].

For the generation of multipartite bound entanglement, a number of schemes have been theoretically proposed and some of them have been experimentally realized. In the discrete-variable regime, a class of four-qubit unlockable bound entangled states, known as the Smolin state, was first proposed in Ref. [25]. Since then, the Smolin state has been deeply studied [5,26] and experimentally demonstrated with polarized photons [27–30] and trapped ions [31]. Here, we focus on the continuous-variable (CV) regime, which yields promising perspectives in unconditional quantum state generation and high-efficiency quantum detection [32]. In order to generate a CV quadripartite unlockable bound entangled state (also named the CV Smolin state), a feasible method is to mix a bipartite entangled state with two external thermal states [6,11,19]. However, the above scheme is limited by the thermal noise introduced into the system. Although the thermal noise can decorrelate the bipartite entangled state and therefore realize the undistillability of the CV Smolin state, it can also degrade the superactivation of the CV Smolin state at the same time [6]. As a result, the CV Smolin state can only be obtained within a relatively restricted range of thermal noise. In this paper, we propose a multipartite entangled state manipulation scheme for generating a CV Smolin state via the internal reconfiguration of a quadripartite entangled state from cascaded four-wave mixing (FWM) processes. Based on the unique structure of the cascaded FWM processes [33–37], our scheme utilizes the local operation and classical communication (LOCC) method to degrade the generated quadripartite entangled state, and therefore realize

*Corresponding author: jxin@hdu.edu.cn

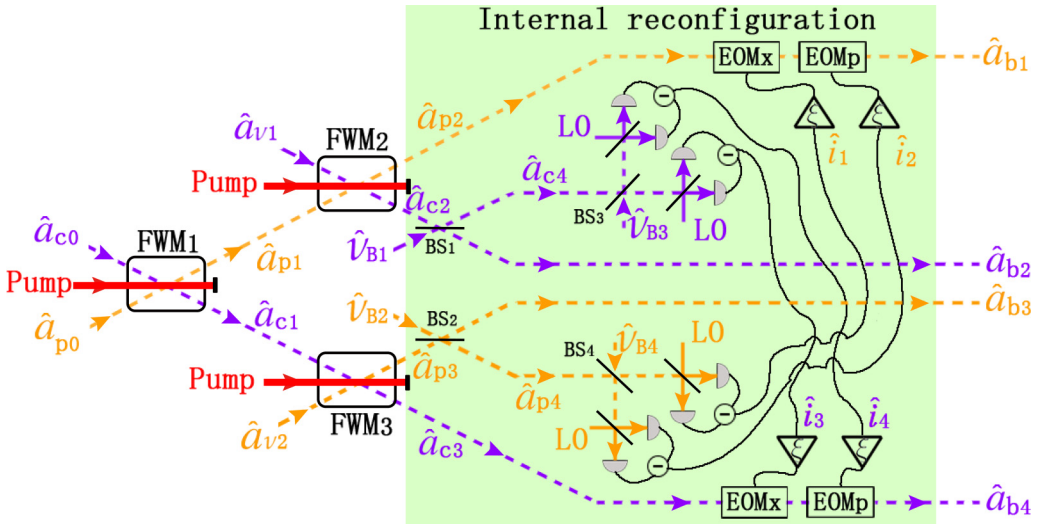

FIG. 1. Scheme for the generation of a CV Smolin state from cascaded FWM processes.

the nondistillability of the CV Smolin state. Furthermore, we also demonstrate the superactivation of the generated CV Smolin state. An Einstein-Podolsky-Rosen (EPR) entangled state can be distilled by employing the tensor product of two identical CV Smolin states generated by our scheme. More importantly, our results show that the CV Smolin state can be obtained by our scheme within a large range of adjustable parameters, which makes it possible to achieve an unconditional CV Smolin state. Our work may provide an idea for the generation of a CV multipartite unlockable bound entangled state.

II. GENERATION OF A CV SMOLIN STATE FROM CASCADED FWM PROCESSES

As is shown in Fig. 1, our scheme for generating a CV Smolin state can be divided into two steps: the generation of a quadripartite entangled state and its internal reconfiguration. For the first step, cascaded FWM processes are used to generate four quantum correlated beams $p2, c2, p3, c3$ that are spatially separated. It has been demonstrated that these beams have strong intensity-difference squeezing [33] and share genuine quadripartite entanglement [34]. The cascaded FWM processes, which consist of three FWM processes, can be theoretically described as follows in detail. When two vacuum states $\hat{a}_{p0}, \hat{a}_{c0}$ enter into the first FWM process (FWM_1) pumped by a strong pump beam (pump), they will be amplified and become $\hat{a}_{p1}, \hat{a}_{c1}$, respectively. The input-output relation for the FWM_1 can be given by

$$\hat{a}_{p1} = G_1\hat{a}_{p0} + g_1\hat{a}^{\dagger}_{c0}, \hat{a}_{c1} = G_1\hat{a}_{c0} + g_1\hat{a}^{\dagger}_{p0}, \qquad (1)$$

where G_1 is the amplitude gain of the FWM_1 and $g_1^2 = G_1^2 - 1$. To generate spatially separated quadripartite entangled beams, the twin beams $p1, c1$ are injected into the second and third FWM processes (FWM_2 and FWM_3), respectively. Then the beams $p1$ and $c1$ are amplified to become $p2$ and $c3$, and two new beams $c2$ and $p3$ are generated. In this way, the FWM_2 (FWM_3) can be expressed as

$$\hat{a}_{p2} = G_2\hat{a}_{p1} + g_2\hat{a}^{\dagger}_{v1}, \quad \hat{a}_{c2} = G_2\hat{a}_{v1} + g_2\hat{a}^{\dagger}_{p1},$$
$$(\hat{a}_{p3} = G_3\hat{a}_{v2} + g_3\hat{a}^{\dagger}_{c1}, \quad \hat{a}_{c3} = G_3\hat{a}_{c1} + g_3\hat{a}^{\dagger}_{v2}), \qquad (2)$$

where $\hat{a}_{v1}, \hat{a}_{v2}$ are the vacuum states, and G_2 and G_3 are the amplitude gains of the FWM_2 and FWM_3, respectively. For simplification, it is assumed that $G_3 = G_2$ in the following discussions.

Up to now, a quadripartite entangled state $\hat{a}_{p2}, \hat{a}_{c2}, \hat{a}_{p3}, \hat{a}_{c3}$ has been generated from the cascaded FWM processes. However, it is not a quadripartite bound entangled state given that quantum entanglement can be unconditionally distilled from this state. To explain this point, the degree of the distillability D is needed to judge whether quantum entanglement can be distilled from the generated quadripartite entangled state with the help of LOCC. For an arbitrary quantum state including four modes $\hat{a}_1, \hat{a}_2, \hat{a}_3, \hat{a}_4$, there are six bipartite scenarios $\hat{a}_1|\hat{a}_2, \hat{a}_1|\hat{a}_3, \hat{a}_1|\hat{a}_4, \hat{a}_2|\hat{a}_3, \hat{a}_2|\hat{a}_4, \hat{a}_3|\hat{a}_4$. For each pair $\hat{a}_i|\hat{a}_j$, we define the degree of the distillability [6],

$$D_X^{ij} = \langle\Delta^2(\hat{X}_i - \hat{X}_j)\rangle + \left\langle\Delta^2\left(\hat{Y}_i + \hat{Y}_j + \zeta_{Xk}^{ij}\hat{Y}_k + \zeta_{Xl}^{ij}\hat{Y}_l\right)\right\rangle,$$
$$D_Y^{ij} = \langle\Delta^2(\hat{Y}_i + \hat{Y}_j)\rangle + \left\langle\Delta^2\left(\hat{X}_i - \hat{X}_j + \zeta_{Yk}^{ij}\hat{X}_k - \zeta_{Yl}^{ij}\hat{X}_l\right)\right\rangle. \qquad (3)$$

Here, $\langle\Delta^2\hat{O}\rangle = \langle\hat{O}^2\rangle - \langle\hat{O}\rangle^2$, $\hat{X} = \hat{a}^{\dagger} + \hat{a}$, and $\hat{Y} = i\hat{a}^{\dagger} - i\hat{a}$ are the amplitude and phase quadratures of the corresponding field. $\zeta_{Xk(l)}^{ij}$ and $\zeta_{Yk(l)}^{ij}$ are the adjustable classical gains in the LOCC protocol for minimizing the corresponding degree of the distillability D_X^{ij} and D_Y^{ij} [39], and subscripts i, j, k, l are unequal numbers among 1, 2, 3, 4. The pair $\hat{a}_i|\hat{a}_j$ is undistillable on the condition that its minimal degree of the distillability is higher than the quantum noise limit (QNL), i.e., $D_X^{ij} > 4$ and $D_Y^{ij} > 4$ [38]. If all six pairs $\hat{a}_1|\hat{a}_2, \hat{a}_1|\hat{a}_3, \hat{a}_1|\hat{a}_4, \hat{a}_2|\hat{a}_3, \hat{a}_2|\hat{a}_4, \hat{a}_3|\hat{a}_4$ are undistillable, a quadripartite bound entangled state is generated. For the four modes $\hat{a}_{p2}, \hat{a}_{c2}, \hat{a}_{p3}, \hat{a}_{c3}$ output from the cascaded FWM processes, it can be easily inferred that quantum entanglement cannot be distilled from the bipartite scenarios

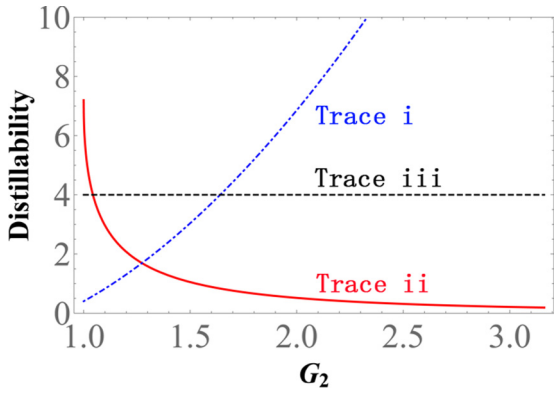

FIG. 2. Distillability of the quadrature entangled state from the cascaded FWM processes. Trace i (blue dash-dotted line) shows the degree of the distillability of the bipartite scenario $\hat{a}_{p2}|\hat{a}_{c3}$, i.e., D_X^{p2c3}, D_Y^{p2c3}, vs G_2. Trace ii (red solid line) shows the degree of the distillability of the bipartite scenarios $\hat{a}_{p2}|\hat{a}_{c2}$, $\hat{a}_{p3}|\hat{a}_{c3}$, i.e., D_X^{p2c2}, D_Y^{p2c2}, D_X^{p3c3}, D_Y^{p3c3}, vs G_2. Trace iii (black dashed line) is the corresponding QNL.

$\hat{a}_{p2}|\hat{a}_{p3}$, $\hat{a}_{c2}|\hat{a}_{c3}$, and $\hat{a}_{c2}|\hat{a}_{p3}$ because these bipartite scenarios consist of the beams which have no interaction with each other [34]. For the other pairs $\hat{a}_{p2}|\hat{a}_{c2}$, $\hat{a}_{p3}|\hat{a}_{c3}$, and $\hat{a}_{p2}|\hat{a}_{c3}$, the minimal degree of the distillability can be easily calculated and given by

$$D_X^{p2c2} = D_Y^{p2c2} = D_X^{p3c3} = D_Y^{p3c3} = \frac{4G_1^4\left(2G_2^2 - 2G_2 g_2 - 1\right)}{G_1^2 + g_1^2},$$
$$D_X^{p2c3} = D_Y^{p2c3} = \frac{4\left(2G_1^2G_2^2 - 2G_1 g_1 G_2^2 - 1\right)\left(1 + 2G_1^2G_2^2 g_2^2\right)}{1 + 4G_1^2G_2^2 g_2^2}. \tag{4}$$

Figure 2 shows the minimal degree of the distillability of the three bipartite scenarios $\hat{a}_{p2}|\hat{a}_{c2}$, $\hat{a}_{p3}|\hat{a}_{c3}$, $\hat{a}_{p2}|\hat{a}_{c3}$ versus G_2 when we fix G_1 at $\sqrt{3}$. As is shown by trace i (blue dash-dotted line) in Fig. 2, it can be found that the degree of the distillability $D_{X(Y)}^{p2c3}$ raises quickly with the increasing of G_2, and $D_{X(Y)}^{p2c3}$ is higher than the QNL when $G_2 > 1.64$. In other words, the FWM_2 and FWM_3 degrade the distillability of the pair $\hat{a}_{p2}|\hat{a}_{c3}$ and we cannot distill the quantum entanglement from the pair $\hat{a}_{p2}|\hat{a}_{c3}$ for any $G_2 > 1.64$. It is because the FWM_2 and FWM_3 introduce added thermal noise into the fields $\hat{a}_{p2}$ and $\hat{a}_{c3}$, respectively. These thermal noise has no quantum correlations and therefore will degrade the quantum entanglement between the fields $\hat{a}_{p2}$ and $\hat{a}_{c3}$. Although the FWM_2 and FWM_3 can make the pair $\hat{a}_{p2}|\hat{a}_{c3}$ undistillable, they will introduce quantum correlations into the other two pairs $\hat{a}_{p2}|\hat{a}_{c2}$ and $\hat{a}_{p3}|\hat{a}_{c3}$, respectively. As is shown by trace ii (red solid line) in Fig. 2, it can be found that for almost all gain range, as long as $G_2 > 1.04$, the degree of the distillability $D_{X(Y)}^{p2c2}$, $D_{X(Y)}^{p3c3}$ is lower than the QNL. It means that the pairs $\hat{a}_{p2}|\hat{a}_{c2}$ and $\hat{a}_{p3}|\hat{a}_{c3}$ are undistillable only under the condition that $G_2 < 1.04$. Traces i and ii cannot be higher than the QNL at the same time and therefore the quantum entanglement can be unconditionally distilled from either the pair $\hat{a}_{p2}|\hat{a}_{c3}$ or the other two pairs $\hat{a}_{p2}|\hat{a}_{c2}$, $\hat{a}_{p3}|\hat{a}_{c3}$. Since the criterion of a quadripartite bound entangled state is that all six bipartite scenarios have to be undistillable simultaneously, the four-mode entangled state $\hat{a}_{p2}, \hat{a}_{c2}, \hat{a}_{p3}, \hat{a}_{c3}$ output from the cascaded FWM processes is not a quadripartite bound entangled state.

In order to realize the undistillability of the quadripartite bound entangled state, decoherent processes have to be introduced into the entanglement system. In this aspect, a serviceable method is to involve external thermal states [6]. Different from the previous scheme, here we propose to decorrelate a quadripartite entangled state by its internal reconfiguration. It has been demonstrated above that the FWM_2 and FWM_3 will introduce the quantum correlations into the pairs $\hat{a}_{p2}|\hat{a}_{c2}$ and $\hat{a}_{p3}|\hat{a}_{c3}$, respectively. However, these two FWM processes are independent and therefore the thermal noise generated by them has no quantum correlations. Along this line, we propose to couple the state $\hat{a}_{p2}$ ($\hat{a}_{c3}$) from the FWM_2 (FWM_3) with the thermal state from the FWM_3 (FWM_2) to decorrelate the pair $\hat{a}_{p2}|\hat{a}_{c2}$ ($\hat{a}_{p3}|\hat{a}_{c3}$) by using LOCC. We call this scheme the internal reconfiguration of the quadripartite entangled state (IRQS) from the cascaded FWM processes, which is highlighted in the green background in Fig. 1. First, we seed two beams $c2$ and $p3$ from the cascaded FWM processes into two 50:50 beam splitters (BS_1 and BS_2), respectively. Then the beam $c2$ is split into $c4$ and $b2$, while the beam $p3$ is split into $b3$ and $p4$. The input-output relation for the BS_1 (BS_2) is given by

$$\hat{a}_{c4} = (\hat{a}_{c2} + \hat{v}_{B1})/\sqrt{2}, \quad \hat{a}_{b2} = (\hat{a}_{c2} - \hat{v}_{B1})/\sqrt{2},$$
$$(\hat{a}_{b3} = (\hat{a}_{p3} - \hat{v}_{B2})/\sqrt{2}, \quad \hat{a}_{p4} = (\hat{a}_{p3} + \hat{v}_{B2})/\sqrt{2}), \tag{5}$$

where $\hat{v}_{B1}$ ($\hat{v}_{B2}$) is the vacuum state. So far, two thermal states $\hat{a}_{c4}$ and $\hat{a}_{p4}$ have been prepared. In order to couple the thermal state $\hat{a}_{c4}$ ($\hat{a}_{p4}$) with the state $\hat{a}_{c3}$ ($\hat{a}_{p2}$), a CV "Bell-state" measurement [39] is used to obtain the information of the amplitude $\hat{X}_{c4}$ ($\hat{X}_{p4}$) and phase quadratures $\hat{Y}_{c4}$ ($\hat{Y}_{p4}$) simultaneously. For the CV Bell-state measurement, first the thermal state $\hat{a}_{c4}$ ($\hat{a}_{p4}$) is seeded into a beam splitter BS_3 (BS_4), where it is assumed that the other port of the BS_3 (BS_4) is in vacuum state $\hat{v}_{B3}$ ($\hat{v}_{B4}$). Then the two output states from the BS_3 (BS_4) are measured by two balanced homodyne detections. Therefore, the amplitude-sum quadrature $\hat{X}_{c4} + \hat{X}_{v_{B3}}$ ($\hat{X}_{p4} + \hat{X}_{v_{B4}}$) and phase-difference quadrature $\hat{Y}_{c4} - \hat{Y}_{v_{B3}}$ ($\hat{Y}_{p4} - \hat{Y}_{v_{B4}}$) can be obtained, which correspond to the output photocurrents of the homodyne detections $\hat{i}_1$ ($\hat{i}_3$) and $\hat{i}_2$ ($\hat{i}_4$), respectively. Then the photocurrents $\hat{i}_1$ ($\hat{i}_3$) and $\hat{i}_2$ ($\hat{i}_4$) are sent to an amplitude electro-optical modulator (EOMx) and a phase electro-optical modulator (EOMp), respectively, to modulate the field $\hat{a}_{p2}$ ($\hat{a}_{c3}$) to become $\hat{a}_{b1}$ ($\hat{a}_{b4}$):

$$\hat{a}_{b1} = \hat{a}_{p2} + \xi_1\hat{i}_1 + i\xi_2\hat{i}_2,$$
$$(\hat{a}_{b4} = \hat{a}_{c3} + \xi_1\hat{i}_3 + i\xi_2\hat{i}_4), \tag{6}$$

where ξ_1 (ξ_3) and ξ_2 (ξ_4) are the adjustable gains in the amplitude and phase modulations. For simplification, it is assumed that $\xi = \xi_1 = \xi_2 = \xi_3 = \xi_4$ in the following discussions. Up to now, the resulting beams $b1, b2, b3, b4$ generated by the IRQS from the cascaded FWM processes are generated. It can be demonstrated that the generated four-mode state $\hat{a}_{b1}, \hat{a}_{b2}, \hat{a}_{b3}, \hat{a}_{b4}$ is a quadripartite bound entangled

state. To demonstrate this point, we need to calculate the degree of the distillability for the six bipartite scenarios $\hat{a}_{b1}|\hat{a}_{b2}, \hat{a}_{b1}|\hat{a}_{b3}, \hat{a}_{b1}|\hat{a}_{b4}, \hat{a}_{b2}|\hat{a}_{b3}, \hat{a}_{b2}|\hat{a}_{b4}, \hat{a}_{b3}|\hat{a}_{b4}$, which is given by

$$D_X^{b1b2} = \left(g_1G_2 + G_1g_2\frac{\zeta_{Xb3}^{b1b2}+\xi}{\sqrt{2}} - G_1G_2\zeta_{Xb4}^{b1b2} - \frac{g_1g_2}{\sqrt{2}} - \frac{g_1g_2\zeta_{Xb4}^{b1b2}\xi}{\sqrt{2}}\right)^2 + \left(G_1G_2 + g_1g_2\frac{\zeta_{Xb3}^{b1b2}+\xi}{\sqrt{2}} - g_1G_2\zeta_{Xb4}^{b1b2} - \frac{G_1g_2}{\sqrt{2}} - \frac{G_1g_2\zeta_{Xb4}^{b1b2}\xi}{\sqrt{2}}\right)^2 + \left(G_1G_2 + g_2\frac{g_1\xi - G_1}{\sqrt{2}}\right)^2 + \left(g_1G_2 + g_2\frac{G_1\xi - g_1}{\sqrt{2}}\right)^2 + \left(g_2\zeta_{Xb4}^{b1b2} - G_2\frac{\zeta_{Xb3}^{b1b2}+\xi}{\sqrt{2}}\right)^2 + \left(g_2 - G_2\frac{1+\zeta_{Xb4}^{b1b2}\xi}{\sqrt{2}}\right)^2 + \frac{\left(\zeta_{Xb4}^{b1b2}\xi - 1\right)^2}{2} + \frac{\left(\zeta_{Xb3}^{b1b2} - \xi\right)^2}{2} + \left(g_2 - \frac{G_2}{\sqrt{2}}\right)^2 + \frac{G_2^2\xi^2}{2} + \left(\zeta_{Xb4}^{b1b2}\xi\right)^2 + \frac{5\xi^2}{2} + \frac{1}{2}, \tag{7}$$

$$D_X^{b1b3} = \left(g_1G_2 + G_1g_2\frac{1+\xi}{\sqrt{2}} - G_1G_2\zeta_{Xb4}^{b1b3} - g_1g_2\frac{\zeta_{Xb2}^{b1b3}+\zeta_{Xb4}^{b1b3}\xi}{\sqrt{2}}\right)^2 + \left(G_1G_2 + g_1g_2\frac{1+\xi}{\sqrt{2}} - g_1G_2\zeta_{Xb4}^{b1b3} - G_1g_2\frac{\zeta_{Xb2}^{b1b3}+\zeta_{Xb4}^{b1b3}\xi}{\sqrt{2}}\right)^2 + \left(G_1G_2 + g_1g_2\frac{\xi-1}{\sqrt{2}}\right)^2 + \left(g_1G_2 + G_1g_2\frac{\xi-1}{\sqrt{2}}\right)^2 + \left(g_2\zeta_{Xb4}^{b1b3} - G_2\frac{1+\xi}{\sqrt{2}}\right)^2 + \left(g_2 - G_2\frac{\zeta_{Xb2}^{b1b3}+\zeta_{Xb4}^{b1b3}\xi}{\sqrt{2}}\right)^2 + G_2^2\frac{(\xi-1)^2}{2} + \frac{\left(\zeta_{Xb4}^{b1b3}\xi - \zeta_{Xb2}^{b1b3}\right)^2}{2} + 3\xi^2 + \left(\zeta_{Xb4}^{b1b3}\xi\right)^2 + g_2^2 + 1, \tag{8}$$

$$D_X^{b1b4} = \left(G_1G_2 + g_1g_2\frac{\zeta_{Xb3}^{b1b4}+\xi}{\sqrt{2}} - g_1G_2 - G_1g_2\frac{\zeta_{Xb2}^{b1b4}+\xi}{\sqrt{2}}\right)^2 + \left(g_1G_2 + G_1g_2\frac{\zeta_{Xb3}^{b1b4}+\xi}{\sqrt{2}} - G_1G_2 - g_1g_2\frac{\zeta_{Xb2}^{b1b4}+\xi}{\sqrt{2}}\right)^2 + \frac{1}{2}(G_1-g_1)^2(\sqrt{2}g_2\xi - 2G_2)^2 + \frac{1}{2}(\sqrt{2}G_2\xi - 2g_2)^2 + \left(g_2 - G_2\frac{\zeta_{Xb2}^{b1b4}+\xi}{\sqrt{2}}\right)^2 + \left(g_2 - G_2\frac{\zeta_{Xb3}^{b1b4}+\xi}{\sqrt{2}}\right)^2 + \frac{\left(\zeta_{Xb2}^{b1b4} - \xi\right)^2}{2} + \frac{\left(\zeta_{Xb3}^{b1b4} - \xi\right)^2}{2} + 5\xi^2, \tag{9}$$

$$D_X^{b2b3} = \left(g_1G_2\zeta_{Xb1}^{b2b3} + G_1g_2\frac{1+\zeta_{Xb1}^{b2b3}\xi}{\sqrt{2}} - G_1G_2\zeta_{Xb4}^{b2b3} - g_1g_2\frac{1+\zeta_{Xb4}^{b2b3}\xi}{\sqrt{2}}\right)^2 + \left(G_1G_2\zeta_{Xb1}^{b2b3} + g_1g_2\frac{1+\zeta_{Xb1}^{b2b3}\xi}{\sqrt{2}} - g_1G_2\zeta_{Xb4}^{b2b3} - G_1g_2\frac{1+\zeta_{Xb4}^{b2b3}\xi}{\sqrt{2}}\right)^2 + \left(g_2\zeta_{Xb4}^{b2b3} - G_2\frac{1+\zeta_{Xb1}^{b2b3}\xi}{\sqrt{2}}\right)^2 + \left(g_2\zeta_{Xb1}^{b2b3} - G_2\frac{1+\zeta_{Xb4}^{b2b3}\xi}{\sqrt{2}}\right)^2 + \frac{\left(\zeta_{Xb1}^{b2b3}\xi - 1\right)^2}{2} + \frac{\left(\zeta_{Xb4}^{b2b3}\xi - 1\right)^2}{2} + \left(\zeta_{Xb1}^{b2b3}\xi\right)^2 + \left(\zeta_{Xb4}^{b2b3}\xi\right)^2 + g_2^2(G_1-g_1)^2 + G_2^2 + 1, \tag{10}$$

$$D_X^{b2b4} = \left(g_1G_2 + G_1g_2\frac{1+\xi}{\sqrt{2}} - G_1G_2\zeta_{Xb1}^{b2b4} - g_1g_2\frac{\zeta_{Xb3}^{b2b4}+\zeta_{Xb1}^{b2b4}\xi}{\sqrt{2}}\right)^2 + \left(G_1G_2 + g_1g_2\frac{1+\xi}{\sqrt{2}} - g_1G_2\zeta_{Xb1}^{b2b4} - G_1g_2\frac{\zeta_{Xb3}^{b2b4}+\zeta_{Xb1}^{b2b4}\xi}{\sqrt{2}}\right)^2 + \left(G_1G_2 + g_1g_2\frac{\xi-1}{\sqrt{2}}\right)^2 + \left(g_1G_2 + G_1g_2\frac{\xi-1}{\sqrt{2}}\right)^2 + \left(g_2\zeta_{Xb1}^{b2b4} - G_2\frac{1+\xi}{\sqrt{2}}\right)^2 + \left(g_2 - G_2\frac{\zeta_{Xb3}^{b2b4}+\zeta_{Xb1}^{b2b4}\xi}{\sqrt{2}}\right)^2 + G_2^2\frac{(\xi-1)^2}{2} + \frac{\left(\zeta_{Xb1}^{b2b4}\xi - \zeta_{Xb3}^{b2b4}\right)^2}{2} + 3\xi^2 + \left(\zeta_{Xb1}^{b2b4}\xi\right)^2 + g_2^2 + 1, \tag{11}$$

$$D_X^{b3b4} = \left(g_1G_2 + G_1g_2\frac{\zeta_{Xb2}^{b3b4}+\xi}{\sqrt{2}} - G_1G_2\zeta_{Xb1}^{b3b4} - \frac{g_1g_2}{\sqrt{2}} - \frac{g_1g_2\zeta_{Xb1}^{b3b4}\xi}{\sqrt{2}}\right)^2 + \left(G_1G_2 + g_1g_2\frac{\zeta_{Xb2}^{b3b4}+\xi}{\sqrt{2}} - g_1G_2\zeta_{Xb1}^{b3b4} - \frac{G_1g_2}{\sqrt{2}} - \frac{G_1g_2\zeta_{Xb1}^{b3b4}\xi}{\sqrt{2}}\right)^2 + \left(G_1G_2 + g_2\frac{g_1\xi - G_1}{\sqrt{2}}\right)^2 + \left(g_1G_2 + g_2\frac{G_1\xi - g_1}{\sqrt{2}}\right)^2 + \left(g_2\zeta_{Xb1}^{b3b4} - G_2\frac{\zeta_{Xb2}^{b3b4}+\xi}{\sqrt{2}}\right)^2 + \left(g_2 - G_2\frac{1+\zeta_{Xb1}^{b3b4}\xi}{\sqrt{2}}\right)^2 + \frac{\left(\zeta_{Xb1}^{b3b4} - 1\right)^2}{2} + \frac{\left(\zeta_{Xb2}^{b3b4} - \xi\right)^2}{2} + \left(g_2 - \frac{G_2}{\sqrt{2}}\right)^2 + \frac{G_2^2\xi^2}{2} + \left(\zeta_{Xb1}^{b3b4}\xi\right)^2 + \frac{5\xi^2}{2} + \frac{1}{2}. \tag{12}$$

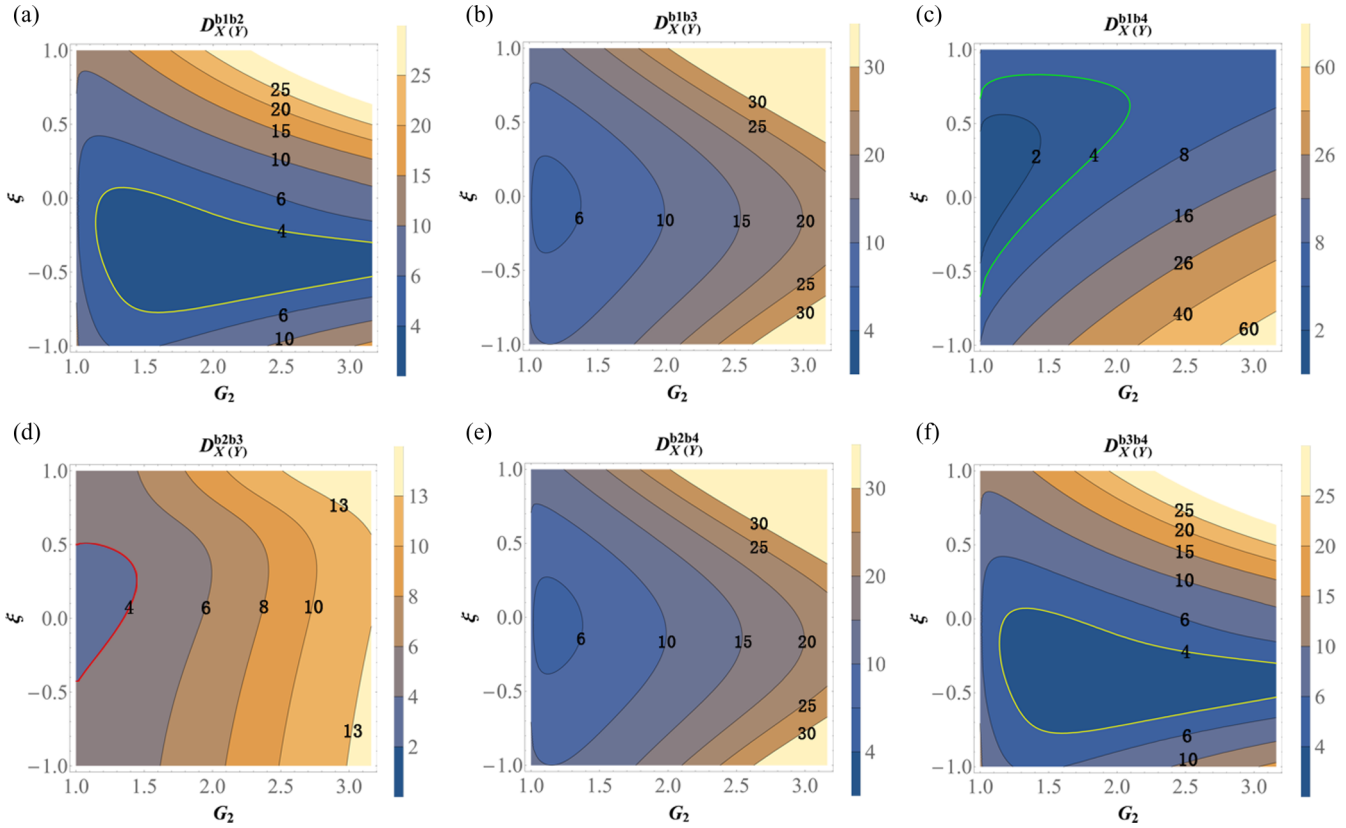

FIG. 3. The contour plots of the minimal degree of the distillability $D^{b1b2}_{X(Y)}$, $D^{b1b3}_{X(Y)}$, $D^{b1b4}_{X(Y)}$, $D^{b2b3}_{X(Y)}$, $D^{b2b4}_{X(Y)}$, $D^{b3b4}_{X(Y)}$, varying with G_2 and ξ.

The degree of the distillability D^{b1b2}_{Y}, D^{b1b3}_{Y}, D^{b1b4}_{Y}, D^{b2b3}_{Y}, D^{b2b4}_{Y}, and D^{b3b4}_{Y} can be obtained by replacing each subscript X with Y in Eqs. (7)–(12), respectively. For the distillability of each bipartite scenario $D^{ij}_{X(Y)}$ in the above equations, we adjust the classical gains $\zeta^{ij}_{X(Y)k}$ and $\zeta^{ij}_{X(Y)l}$ (see Appendix A for details) in the LOCC protocol as mentioned in Eq. (3) to achieve its minimal value, which becomes a function of ξ and G_2 later. The contour plots of the minimal degree of the distillability $D^{b1b2}_{X(Y)}$, $D^{b1b3}_{X(Y)}$, $D^{b1b4}_{X(Y)}$, $D^{b2b3}_{X(Y)}$, $D^{b2b4}_{X(Y)}$, $D^{b3b4}_{X(Y)}$ are shown in Figs. 3(a)–3(f), respectively, where it is assumed that the gain of the FWM$_1$ $G_1 = \sqrt{3}$. We first focus on the pair $\hat{a}_{b1}|\hat{a}_{b2}$, and its minimal distillability $D^{b1b2}_{X(Y)}$ is shown in Fig. 3(a). It is clear that for any G_2 from 1 to $\sqrt{10}$, we can always make the minimal distillability $D^{b1b2}_{X(Y)} > 4$ by adjusting ξ. This interesting result is very different from that of the pair $\hat{a}_{p2}|\hat{a}_{c2}$, which is the precursor of the pair $\hat{a}_{b1}|\hat{a}_{b2}$ before the IRQS from the cascaded FWM processes as shown in Fig. 1. For the pair $\hat{a}_{p2}|\hat{a}_{c2}$, as shown by trace ii in Fig. 2, it has been demonstrated that its minimal distillability $D^{p2c2}_{X(Y)} > 4$ is limited by $1 < G_2 < 1.04$. The reason why the scheme IRQS can enlarge the undistillable range of the pair $\hat{a}_{p2}|\hat{a}_{c2}$ is that it couples the thermal state $\hat{a}_{p4}$ from the FWM$_3$ with the state $\hat{a}_{p2}$, and therefore decorrelates the pair $\hat{a}_{p2}|\hat{a}_{c2}$. For other pairs, it can be found that the contour plot of the minimal distillability $D^{b1b2}_{X(Y)}$ [as shown in Fig. 3(a)] is exactly the same as the one of $D^{b3b4}_{X(Y)}$ [as shown in Fig. 3(f)], while $D^{b1b3}_{X(Y)}$ [as shown in Fig. 3(b)] is the same with $D^{b2b4}_{X(Y)}$ [as shown in Fig. 3(e)], which is due to the symmetry of the four-mode state $\hat{a}_{b1}, \hat{a}_{b2}, \hat{a}_{b3}, \hat{a}_{b4}$ generated by the IRQS from the cascaded FWM processes. As shown in Figs. 3(b) and 3(e), the minimal distillability $D^{b1b3}_{X(Y)}$ and $D^{b2b4}_{X(Y)}$ is always larger than 4, i.e., the quantum entanglement can never be distilled from the pairs $\hat{a}_{b1}|\hat{a}_{b3}$ and $\hat{a}_{b2}|\hat{a}_{b4}$. For the other four pairs $\hat{a}_{b1}|\hat{a}_{b2}$, $\hat{a}_{b1}|\hat{a}_{b4}$, $\hat{a}_{b2}|\hat{a}_{b3}$, $\hat{a}_{b3}|\hat{a}_{b4}$, they cannot be undistillable all the time, but have their own undistillable regions (the regions where the minimal degree of the distillability is larger than 4), which is bounded by yellow, green, red, and yellow curves as shown in Figs. 3(a), 3(c), 3(d), and 3(f), respectively. Since a quadripartite bound entangled state yields that all its six bipartite scenarios have to be undistillable, the overlap of the undistillable regions of the pairs $\hat{a}_{b1}|\hat{a}_{b2}$, $\hat{a}_{b1}|\hat{a}_{b4}$, $\hat{a}_{b2}|\hat{a}_{b3}$, $\hat{a}_{b3}|\hat{a}_{b4}$ gives the regions of the quadripartite bound entangled state generated by the IRQS from the cascaded FWM processes, which are shown by the black shallow regions R_{B1} and R_{B2} in Fig. 4. It can be found that the quadripartite bound entangled state in our system can be achieved in a wide range with the change of G_2 and ξ. For any $G_2 > 1$, there always exists suitable ξ making the four-mode entangled state from the cascaded FWM processes become a quadripartite bound entangled state. Furthermore, when ξ is fixed within some special range, i.e., $\xi < -0.77$ or $\xi > 0.83$, a quadripartite bound entangled state can be unconditionally obtained from our system, whatever G_2 is.

The four-mode state generated by the IRQS from the cascaded FWM processes is not only undistillable but also unlockable, which makes it become a quadripartite unlockable bound entangled state (also named CV Smolin

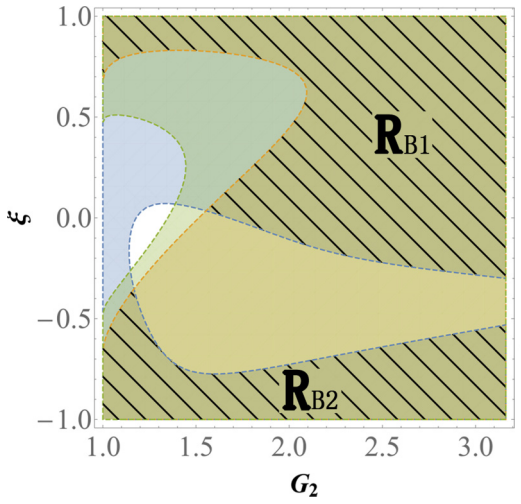

FIG. 4. The regions of the quadripartite bound entangled state generated by the IRQS from the cascaded FWM processes.

state). It is well known that a quadripartite bound entangled state is undistillable when its four modes remain spatially separated from each other. However, an EPR entangled state can be distilled by the superactivation (or unlockability) protocol, in which the tensor product of two identical CV Smolin states has to be employed [5]. The superactivation protocol of two identical CV Smolin states is shown by the inset in the upper left of Fig. 5. First, there are two copies of CV Smolin states $\hat{a}_{b1}, \hat{a}_{b2}, \hat{a}_{b3}, \hat{a}_{b4}$ and $\hat{a}_{b5}, \hat{a}_{b6}, \hat{a}_{b7}, \hat{a}_{b8}$ from which no quantum entanglement can be distilled. We divide these two CV Smolin states into five parties A, B, C, D, E which consist of $(\hat{a}_{b1})$, $(\hat{a}_{b2}, \hat{a}_{b5})$, $(\hat{a}_{b3}, \hat{a}_{b6})$, $(\hat{a}_{b4}, \hat{a}_{b7})$, and $(\hat{a}_{b8})$, respectively. Then, joint quantum measurements are performed in the parties B–D, respectively, and all measured

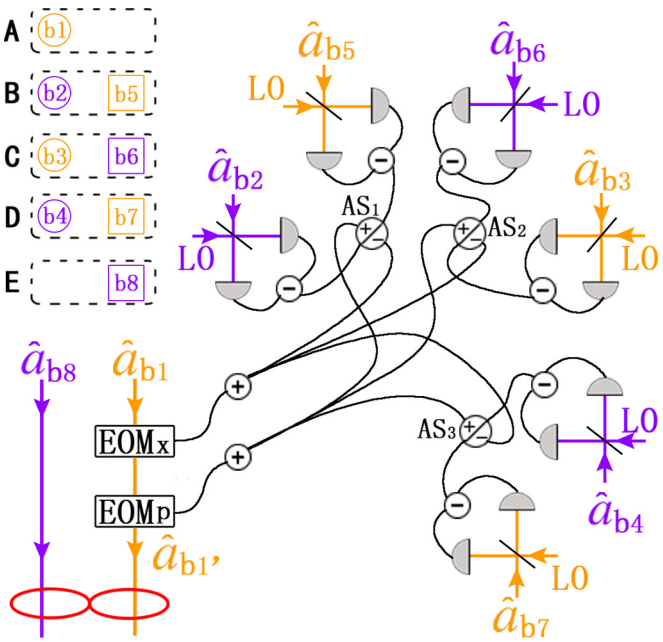

FIG. 5. The scheme for superactivating two identical CV Smolin states.

outcomes are sent to party A. Finally, an EPR entangled state can be distilled between the two parties A and E. A detailed scheme for superactivating two identical CV Smolin states is shown in Fig. 5, where $\hat{a}_{b1}, \hat{a}_{b2}, \hat{a}_{b3}, \hat{a}_{b4}$ and $\hat{a}_{b5}, \hat{a}_{b6}, \hat{a}_{b7}, \hat{a}_{b8}$ are two identical quadripartite bound entangled states generated by the scheme IRQSs from two sets of the cascaded FWM processes. For each of the parties $(\hat{a}_{b2}, \hat{a}_{b5})$, $(\hat{a}_{b3}, \hat{a}_{b6})$, and $(\hat{a}_{b4}, \hat{a}_{b7})$, joint homodyne detection is performed to obtain both its sum-phase and difference-amplitude quadratures $(\hat{Y}_{b2} + \hat{Y}_{b5}$ and $\hat{X}_{b2} - \hat{X}_{b5})$, $(\hat{Y}_{b3} + \hat{Y}_{b6}$ and $\hat{X}_{b3} - \hat{X}_{b6})$, and $(\hat{Y}_{b4} + \hat{Y}_{b7}$ and $\hat{X}_{b4} - \hat{X}_{b7})$, which correspond to the photocurrents $(\hat{i}^{+}_{AS_1}$ and $\hat{i}^{-}_{AS_1})$, $(\hat{i}^{+}_{AS_2}$ and $\hat{i}^{-}_{AS_2})$, and $(\hat{i}^{+}_{AS_3}$ and $\hat{i}^{-}_{AS_3})$ output from the adder and subtractor AS_1, AS_2, and AS_3. Then all the photocurrents from the adders (subtractors) are summed up and the sum current is sent to the EOMp (EOMx) to modulate the field $\hat{a}_{b1}$ to become $\hat{a}_{b1'}$. As a result, the field $\hat{a}_{b1'}$ can be expressed as

$$\hat{a}_{b1'} = \hat{a}_{b1} + \kappa_1 \hat{i}^{-}_{AS_1} + \kappa_2 \hat{i}^{-}_{AS_2} + \kappa_3 \hat{i}^{-}_{AS_3} + i\kappa_1 \hat{i}^{+}_{AS_1} + i\kappa_2 \hat{i}^{+}_{AS_2} + i\kappa_3 \hat{i}^{+}_{AS_3}, \tag{13}$$

where κ_1, κ_2, and κ_3 are the adjustable gains for the photocurrents' output from the AS_1, AS_2, and AS_3, respectively. In order to verify the superactivation process, the degree of the entanglement between the two fields, $\hat{a}_{b1'}$ and $\hat{a}_{b8}$, should be analyzed, which can be quantified by the inseparability parameter $I_{b1'b8} = \langle \Delta^2(\hat{X}_{b1'} - \hat{X}_{b8}) \rangle + \langle \Delta^2(\hat{Y}_{b1'} + \hat{Y}_{b8}) \rangle$ [40,41]. The two-mode state $\hat{a}_{b1'}$ and $\hat{a}_{b8}$ is an EPR entangled state on the condition that $I_{b1'b8} < 4$. It can be calculated that

$$\begin{aligned} I_{b1'b8} = {} & 4\left(g_1 G_2 + G_1 g_2 \frac{\xi - \kappa_2}{\sqrt{2}} - G_1 G_2 \kappa_1 - g_1 g_2 \frac{\kappa_1 \xi + \kappa_3}{\sqrt{2}}\right)^2 \\ & + 4\left(G_1 G_2 + g_1 g_2 \frac{\xi - \kappa_2}{\sqrt{2}} - g_1 G_2 \kappa_1 - G_1 g_2 \frac{\kappa_1 \xi + \kappa_3}{\sqrt{2}}\right)^2 \\ & + 4\left(g_2 \kappa_1 + G_2 \frac{\kappa_2 - \xi}{\sqrt{2}}\right)^2 + 4\left(g_2 - G_2 \frac{\kappa_1 \xi + \kappa_3}{\sqrt{2}}\right)^2 \\ & + 2(\kappa_1 \xi - \kappa_3)^2 + 2(\kappa_2 + \xi)^2 + 4\kappa_1^2 \xi^2 + 4\xi^2. \end{aligned} \tag{14}$$

By adjusting $\kappa_1, \kappa_2, \kappa_3$ (see Appendix A for details), we can obtain the minimal inseparability $I_{b1'b8}$ varying with G_2 and ξ, as shown in Fig. 6(a). It can be found that for any $G_2 > 1$, there always exists suitable ξ making the minimal inseparability $I_{b1'b8}$ smaller than 4. That is to say, the two-mode state $\hat{a}_{b1'}, \hat{a}_{b8}$ can always be an EPR entangled state by adjusting ξ. Moreover, when ξ is fixed at some special values ranging from 0 to 0.47, the minimal inseparability $I_{b1'b8}$ can be unconditionally smaller than 4, whatever G_2 is. Therefore, the superactivation of the quadripartite unlockable bound entangled state generated by the IRQS from the cascaded FWM processes is demonstrated.

Since a CV Smolin state yields both the superactivation (or unlockability) and undistillability, the regions of the CV Smolin state generated by the scheme IRQS are the overlap of the unlockable regions [i.e., the regions that the minimal inseparability $I_{b1'b8} > 4$ in Fig. 6(a)] and the undistillable regions (i.e., the black shallow regions in Fig. 4), which is shown by the black shallow regions R_{S1}, R_{S2}, R_{S3} in Fig. 6(b). It can be found that for our system, the CV

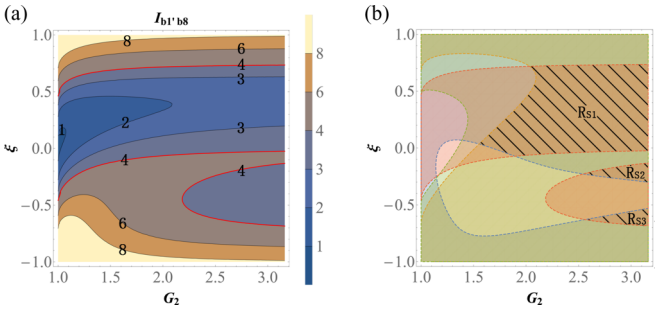

FIG. 6. (a) The contour plot of the minimal inseparability $I_{b1'b8}$ varying with G_2 and ξ. (b) The regions of the CV Smolin state generated by the IRQS from the cascaded FWM processes.

Smolin state can be obtained on the condition that $1.56 < G_2 < \sqrt{10}$, which is an experimentally feasible range. Furthermore, it can be demonstrated that the upper bound of this range can be expanded to ∞. For example, when $\xi = 0.02$, a CV Smolin state can be unconditionally generated by the IRQS from the cascaded FWM processes for any $G_2 > 1.56$.

III. CONCLUSION AND DISCUSSION

A multipartite unlockable bound entangled state, which owns both the undistillability and superactivation, serves as an useful quantum resource in quantum cryptography and quantum teleportation. To generate a CV quadripartite unlockable bound entangled state, also known as the CV Smolin state, a serviceable method is to employ a bipartite entangled state and mix it with two thermal states on beam splitters (BSs) [6,11,19]. However, for a given quadripartite entangled state, how can we make it become a CV Smolin state? In this paper, we have proposed a scheme named IRQS to prepare a CV Smolin state using a quadripartite entangled state. By internally reconfiguring a four-mode entangled state generated from the cascaded FWM processes with the help of LOCC, both the undistillability and superactivation of the CV Smolin state have been demonstrated. More importantly, our results show that the CV Smolin state can be obtained within a large range of adjustable parameters. For example, when $G_1 = \sqrt{3}$ and $\xi = 0.02$, a CV Smolin state can be unconditionally achieved for any $G_2 > 1.56$. In this sense, our scheme has an advantage in obtaining an unconditional CV Smolin state, compared with the previous scheme [6] involving external thermal noise where the CV Smolin state can only be obtained within a relatively restricted range (see Appendix B for details). Given the good scalability of the cascaded FWM processes, if we extend our system with more FWM processes cascaded [33], the IRQS can also be applied to generate a multipartite unlockable bound entangled state with a larger number of mode. In this sense, our work may provide a thought for generating a multipartite unlockable bound entangled state.

ACKNOWLEDGMENTS

This work was supported by the Natural Science Foundation of Zhejiang Province of China (Grants No. LQ19A040008 and No. LY18A050003), the National Natural Science Foundation of China (Grants No. 61871162, No. 11874155, No. 11805048, No. 11847044, No. 91436211, No. 11374104, and No. 10974057), the Natural Science Foundation of Shanghai (Grant No. 17ZR1442900), the Program of Scientific and Technological Innovation of Shanghai (Grant No. 17JC1400401), the Program for Professor of Special Appointment (Eastern Scholar) at Shanghai Institutions of Higher Learning, the National Basic Research Program of China (Grant No. 2016YFA0302103), the 111 project (Grant No. B12024), the Fundamental Research Funds for the Central Universities, and the Program of State Key Laboratory of Advanced Optical Communication Systems and Networks (Grant No. 2018GZKF03006).

APPENDIX A

In order to demonstrate the undistillability of the CV quadripartite unlockable bound entangled state $\hat{a}_{b1}, \hat{a}_{b2}, \hat{a}_{b3}, \hat{a}_{b4}$ generated by our system, we have to analyze the distillability for all six bipartite scenarios $\hat{a}_1|\hat{a}_2$, $\hat{a}_1|\hat{a}_3$, $\hat{a}_1|\hat{a}_4$, $\hat{a}_2|\hat{a}_3$, $\hat{a}_2|\hat{a}_4$, $\hat{a}_3|\hat{a}_4$ given by Eqs. (7)–(12). For each bipartite scenario $\hat{a}_i|\hat{a}_j$, we adjust the classical parameters $\zeta^{ij}_{Xk(l)}, \zeta^{ij}_{Yk(l)}$ in the LOCC to minimize the corresponding distillability $D^{ij}_{X(Y)}$. The contour plots of the minimal distillability $D^{b1b2}_{X(Y)}, D^{b1b3}_{X(Y)}, D^{b1b4}_{X(Y)}, D^{b2b3}_{X(Y)}, D^{b2b4}_{X(Y)}, D^{b3b4}_{X(Y)}$ have been shown in Figs. 3(a)–3(f), respectively. Here, we give their corresponding optimal parameters $(\zeta^{b1b2}_{X(Y)b3}, \zeta^{b1b2}_{X(Y)b4})$, $(\zeta^{b1b3}_{X(Y)b2}, \zeta^{b1b3}_{X(Y)b4})$, $(\zeta^{b1b4}_{X(Y)b2}, \zeta^{b1b4}_{X(Y)b3})$, $(\zeta^{b2b3}_{X(Y)b1}, \zeta^{b2b3}_{X(Y)b4})$, $(\zeta^{b2b4}_{X(Y)b1}, \zeta^{b2b4}_{X(Y)b3})$, $(\zeta^{b3b4}_{X(Y)b1}, \zeta^{b3b4}_{X(Y)b2})$ varying with G_2 and ξ, which are shown in Fig. 7.

In the superactivation protocol, two copies of CV quadripartite unlockable bound entangled states $(\hat{a}_{b1}, \hat{a}_{b2}, \hat{a}_{b3}, \hat{a}_{b4})$, $(\hat{a}_{b5}, \hat{a}_{b6}, \hat{a}_{b7}, \hat{a}_{b8})$ are involved, as shown in Fig. 5. For the pairs $(\hat{a}_{b2}|\hat{a}_{b5})$, $(\hat{a}_{b3}|\hat{a}_{b6})$, $(\hat{a}_{b4}|\hat{a}_{b7})$, joint homodyne detections are used to measure their corresponding sum-phase and difference-amplitude quadratures $(\hat{Y}_{b2} + \hat{Y}_{b5}$ and $\hat{X}_{b2} - \hat{X}_{b5})$, $(\hat{Y}_{b3} + \hat{Y}_{b6}$ and $\hat{X}_{b3} - \hat{X}_{b6})$, and $(\hat{Y}_{b4} + \hat{Y}_{b7}$ and $\hat{X}_{b4} - \hat{X}_{b7})$. Then, all the photocurrents from the joint homodyne detections are used to modulate the field $\hat{a}_{b1}$ to become $\hat{a}_{b1'}$, which has been discussed in Eq. (13). By adjusting the gains of the photocurrents $\kappa_1, \kappa_2, \kappa_3$, we obtain the contour plot of the minimal inseparability $I_{b1'b8}$, as shown in Fig. 6(a). Here, we give the corresponding optimal gains $\kappa_1, \kappa_2, \kappa_3$ varying with G_2 and ξ, which are shown in Fig. 8.

APPENDIX B

In addition to the IRQS as has been proposed in this paper, another feasible method to generate a CV Smolin state is to mix a bipartite entangled state with two thermal states (MBTS), as shown in Fig. 9. The FWM_1 is used to generate a bipartite entangled state $\hat{a}_{p4}$ and $\hat{a}_{c5}$. The FWM_2 and FWM_3 are used to generate thermal states $\hat{a}_{c4}$ and $\hat{a}_{p5}$, respectively. The noise level of the thermal states can be controlled by the gains (G_2 and G_3) of the FWM_2 and FWM_3. It can be derived that the output states from the BSs can be

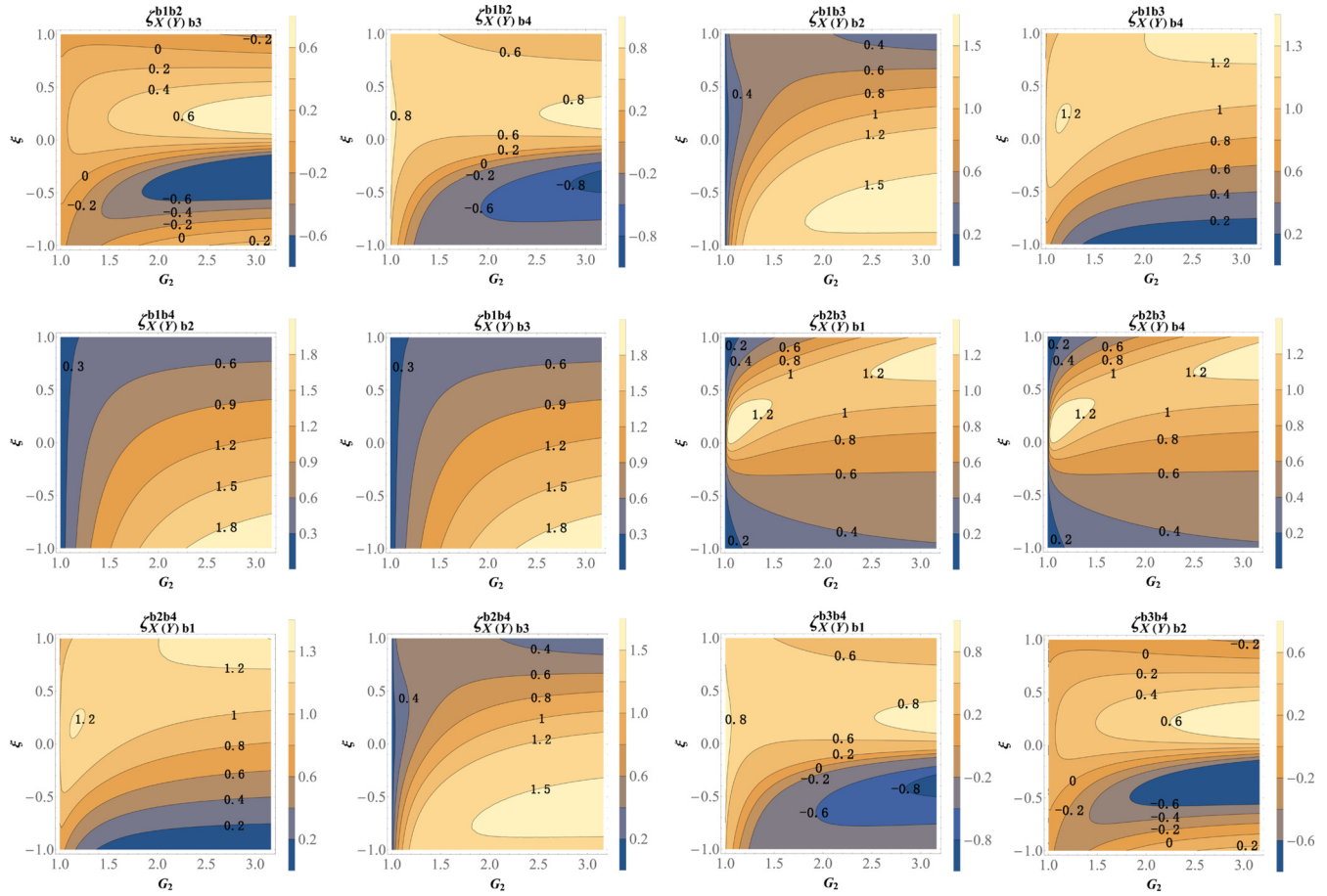

FIG. 7. The subgraphs are sequentially arranged to show the optimal gains $\zeta^{b1b2}_{X(Y)b3}$, $\zeta^{b1b2}_{X(Y)b4}$, $\zeta^{b1b3}_{X(Y)b2}$, $\zeta^{b1b3}_{X(Y)b4}$, $\zeta^{b1b4}_{X(Y)b2}$, $\zeta^{b1b4}_{X(Y)b3}$, $\zeta^{b2b3}_{X(Y)b1}$, $\zeta^{b2b3}_{X(Y)b4}$, $\zeta^{b2b4}_{X(Y)b1}$, $\zeta^{b2b4}_{X(Y)b3}$, $\zeta^{b3b4}_{X(Y)b1}$, $\zeta^{b3b4}_{X(Y)b2}$ varying with G_2 and ξ for minimizing the distillability $D^{b1b2}_{X(Y)}$, $D^{b1b3}_{X(Y)}$, $D^{b1b4}_{X(Y)}$, $D^{b2b3}_{X(Y)}$, $D^{b2b4}_{X(Y)}$, $D^{b3b4}_{X(Y)}$.

expressed as

$$\begin{aligned}
\hat{a}_{b1} &= \frac{1}{\sqrt{2}}(G_1\hat{a}_{p1} + g_1\hat{a}^{\dagger}_{c1} + G_2\hat{a}_{p2} + g_2\hat{a}^{\dagger}_{c2}),\\
\hat{a}_{b2} &= \frac{1}{\sqrt{2}}(G_1\hat{a}_{p1} + g_1\hat{a}^{\dagger}_{c1} - G_2\hat{a}_{p2} - g_2\hat{a}^{\dagger}_{c2}),\\
\hat{a}_{b3} &= \frac{1}{\sqrt{2}}(G_1\hat{a}_{c1} + g_1\hat{a}^{\dagger}_{p1} + G_3\hat{a}_{c3} + g_3\hat{a}^{\dagger}_{p3}),\\
\hat{a}_{b4} &= \frac{1}{\sqrt{2}}(G_1\hat{a}_{c1} + g_1\hat{a}^{\dagger}_{p1} - G_3\hat{a}_{c3} - g_3\hat{a}^{\dagger}_{p3}), \qquad \text{(B1)}
\end{aligned}$$

where $\hat{a}_{p1}, \hat{a}_{p2}, \hat{a}_{p3}, \hat{a}_{c1}, \hat{a}_{c2}, \hat{a}_{c3}$ are the vacuum states. We first study the undistillability of the generated four-mode state $\hat{a}_{b1}, \hat{a}_{b2}, \hat{a}_{b3}, \hat{a}_{b4}$. Obviously, bipartite entanglement between $\hat{a}_{b1}$ and $\hat{a}_{b2}$ as well as $\hat{a}_{b3}$ and $\hat{a}_{b4}$ cannot be obtained by LOCC. This is because each pair of $\hat{a}_{b1}|\hat{a}_{b2}$ and $\hat{a}_{b3}|\hat{a}_{b4}$ is generated by mixing a submode of a bipartite entangled state and a thermal state on a 50:50 BS, and therefore there is no quantum correlation between them. Given the symmetric structure of the system, it can be demonstrated that the undistillability of the generated four-mode state can be obtained on the condition that one of the minimal distillabilities of the four bipartite scenarios $\hat{a}_{b1}|\hat{a}_{b3}$, $\hat{a}_{b1}|\hat{a}_{b4}$, $\hat{a}_{b2}|\hat{a}_{b3}$, $\hat{a}_{b2}|\hat{a}_{b4}$ is

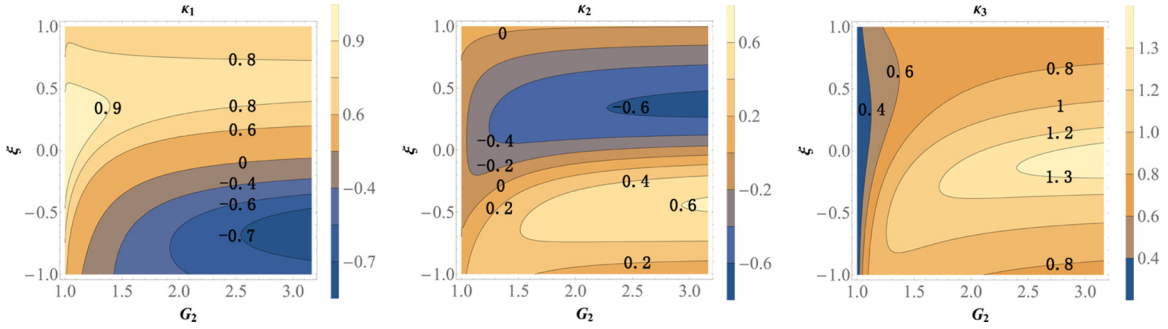

FIG. 8. The subgraphs show the optimal gains $\kappa_1, \kappa_2, \kappa_3$ varying with G_2 and ξ for minimizing the inseparability $I_{b1'b8}$.

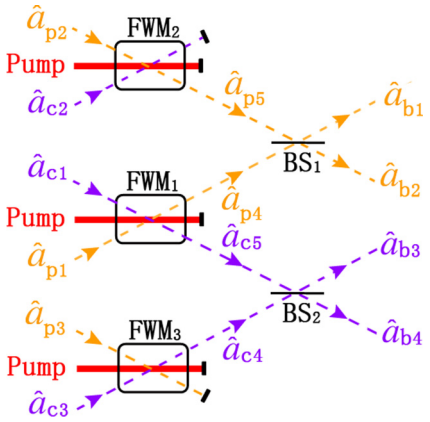

FIG. 9. Scheme for the generation of a CV Smolin state by mixing a bipartite entangled state with two thermal states.

larger than 4. Here we take the bipartite scenario $\hat{a}_{b1}|\hat{a}_{b3}$ as an example. By using Eq. (3), it can be derived that

$$\begin{aligned} D_X^{b1b3} &= \tfrac{1}{2}\left(G_2^2+g_2^2 y\right)\left[\left(1-\zeta_{Xb2}^{b1b3}\right)^2+\left(1-\zeta_{Xb4}^{b1b3}\right)^2\right] \\ &+(G_1-g_1)^2+G_2^2+g_2^2+\tfrac{1}{2}\left[G_1\left(1+\zeta_{Xb2}^{b1b3}\right)\right. \\ &\left.-g_1\left(1+\zeta_{Xb4}^{b1b3}\right)\right]^2+\tfrac{1}{2}\left[G_1\left(1+\zeta_{Xb4}^{b1b3}\right)\right. \\ &\left.-g_1\left(1+\zeta_{Xb2}^{b1b3}\right)\right]^2, \end{aligned} \tag{B2}$$

where ζ_{Xb2}^{b1b3} and ζ_{Xb4}^{b1b3} are the adjustable classical gains in the LOCC protocol for minimizing D_X^{b1b3}. For simplification, it is assumed that $G_3 = G_2$. The degree of the distillability D_Y^{b1b3} can be obtained by replacing each subscript X with Y in Eq. (B2). The minimal degree of $D_{X(Y)}^{b1b3}$ versus G_2 with optimal $\zeta_{X(Y)b2}^{b1b3}$ and $\zeta_{X(Y)b4}^{b1b3}$ taken is shown by trace i (red solid line) in Fig. 10(a), where it is assumed that $G_1 = 1.46$. It can be found that the four-mode state $\hat{a}_{b1}, \hat{a}_{b2}, \hat{a}_{b3}, \hat{a}_{b4}$ is undistillable unless $G_2 > 1.44$. It means that in order to achieve the undistillability of the CV Smolin state, enough thermal noise is required to decorrelate the system. However, the introduced thermal noise will degrade the superactivation of the CV Smolin state. By using the superactivation protocol as shown in Fig. 5, it can be derived that

$$\begin{aligned} I_{b1'b8} &= 2(G_1-\kappa_1 g_1-\kappa_2 g_1-\kappa_3 G_1)^2 \\ &+2\left(G_2^2+g_2^2\right)(1+\kappa_3)^2+2(g_1-\kappa_1 G_1-\kappa_2 G_1 \\ &-\kappa_3 g_1)^2+2\left(G_2^2+g_2^2\right)(\kappa_1-\kappa_2)^2. \end{aligned} \tag{B3}$$

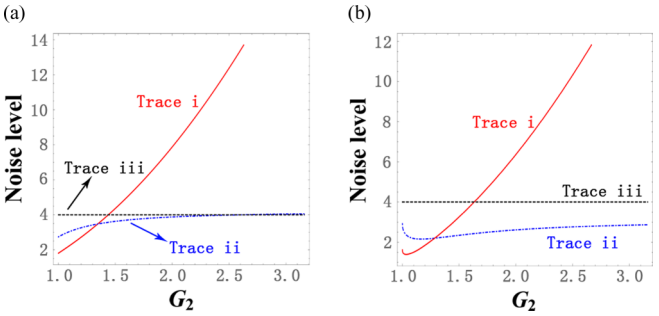

FIG. 10. Comparison between the regions of the CV Smolin state generated by the (a) MBTS and (b) IRQS.

The superactivation of the CV Smolin state can be obtained on the condition that $I_{b1'b8} < 4$. By adjusting $\kappa_1, \kappa_2, \kappa_3$, we can plot the minimal inseparability $I_{b1'b8}$ varying with G_2 as shown by trace ii (blue dash-dotted line) in Fig. 10(a), where it is assumed that $G_1 = 1.46$. Trace iii (black dashed line) is the corresponding QNL. It is clear that the minimal value of $I_{b1'b8}$ becomes larger with the increasing of G_2. In other words, the superactivation of the CV Smolin state generated by the MBTS becomes worse with the increasing of the thermal noise introduced into the system, and when $G_2 > 2.59$ the superactivation of the CV Smolin state generated by the MBTS disappears. By combining both the undistillability and the superactivation together, the CV Smolin state generated by the MBTS can be obtained within the regions of $1.44 < G_2 < 2.59$, which is a relatively restricted range. On the other hand, the CV Smolin state generated by the IRQS can be obtained in a larger range. Since both ξ and G_2 can affect the regions of the CV Smolin state in the IRQS, here we fix $\xi = 0.25$ and treat G_2 as a variable in the following discussions, for simplification. By taking $G_1 = 1.46$ into Eqs. (7)–(13) and (14), the regions of the undistillability and the superactivation of the CV Smolin state generated by the IRQS versus G_2 can be shown by trace i (red solid line) and trace ii (blue dash-dotted line) in Fig. 10(b), respectively. It can be found that regions of the undistillability of the CV Smolin state are obtained as long as $G_2 > 1.63$. More interestingly, the superactivation of the CV Smolin state can be unconditionally achieved for any $G_2 > 1$. As a result, the regions of the CV Smolin state generated by the IRQS are $G_2 > 1.63$, which is a larger range compared with the one of the MBTS.

[1] R. Horodecki, P. Horodecki, M. Horodecki, and K. Horodecki, Rev. Mod. Phys. **81**, 865 (2009).

[2] C. H. Bennett, G. Brassard, S. Popescu, B. Schumacher, J. A. Smolin, and W. K. Wootters, Phys. Rev. Lett. **76**, 722 (1996).

[3] D. Deutsch, A. Ekert, R. Jozsa, C. Macchiavello, S. Popescu, and A. Sanpera, Phys. Rev. Lett. **77**, 2818 (1996).

[4] M. Horodecki, P. Horodecki, and R. Horodecki, Phys. Rev. Lett. **80**, 5239 (1998).

[5] P. W. Shor, J. A. Smolin, and A. V. Thapliyal, Phys. Rev. Lett. **90**, 107901 (2003).

[6] X. Jia, J. Zhang, Y. Wang, Y. Zhao, C. Xie, and K. Peng, Phys. Rev. Lett. **108**, 190501 (2012).

[7] P. Horodecki and M. Lewenstein, Phys. Rev. Lett. **85**, 2657 (2000).

[8] R. Sengupta and Arvind, Phys. Rev. A **84**, 032328 (2011)

[9] F. E. S. Steinhoff, M. C. de Oliveira, J. Sperling, and W. Vogel, Phys. Rev. A **89**, 032313 (2014).

[10] G. Wang and M. Ying, Phys. Rev. A **75**, 052332 (2007).

[11] Jing Zhang, Phys. Rev. A **83**, 052327 (2011).

[12] L. Masanes, Phys. Rev. Lett. **97**, 050503 (2006).

[13] T. Vértesi and N. Brunner, Phys. Rev. Lett. **108**, 030403 (2012).
[14] K. F. Pál and T. Vértesi, Phys. Rev. A **96**, 022123 (2017).
[15] K. Horodecki, M. Horodecki, P. Horodecki, and J. Oppenheim, Phys. Rev. Lett. **94**, 160502 (2005).
[16] I. Chattopadhyay and D. Sarkar, Phys. Lett. A **365**, 273 (2007).
[17] K. Horodecki, Ł. Pankowski, M. Horodecki, and P. Horodecki, IEEE Trans. Inf. Theory **54**, 2621 (2008).
[18] M. Ozols, G. Smith, and J. A. Smolin, Phys. Rev. Lett. **112**, 110502 (2014).
[19] Y. Zhou, J. Yu, Z. Yan, X. Jia, J. Zhang, C. Xie, and K. Peng, Phys. Rev. Lett. **121**, 150502 (2018).
[20] N. Linden and S. Popescu, Phys. Rev. A **59**, 137 (1999).
[21] L. Masanes, Phys. Rev. Lett. **96**, 150501 (2006).
[22] Ł. Czekaj, A. Przysiężna, M. Horodecki, and P. Horodecki, Phys. Rev. A **92**, 062303 (2015).
[23] M. Murao and V. Vedral, Phys. Rev. Lett. **86**, 352 (2001).
[24] M. Epping and Č. Brukner, Phys. Rev. A **87**, 032305 (2013).
[25] J. A. Smolin, Phys. Rev. A **63**, 032306 (2001).
[26] R. Augusiak and P. Horodecki, Phys. Rev. A **73**, 012318 (2006).
[27] E. Amselem and M. Bourennane, Nat. Phys. **5**, 748 (2009).
[28] J. Lavoie, R. Kaltenbaek, M. Piani, and K. J. Resch, Phys. Rev. Lett. **105**, 130501 (2010).
[29] F. Kaneda, R. Shimizu, S. Ishizaka, Y. Mitsumori, H. Kosaka, and K. Edamatsu, Phys. Rev. Lett. **109**, 040501 (2012).
[30] K. Dobek, M. Karpiński, R. Demkowicz-Dobrzański, K. Banaszek, and P. Horodecki, Laser Phys. **23**, 025204 (2013).
[31] J. T. Barreiro, P. Schindler, O. Gühne, T. Monz, M. Chwalla, C. F. Roos, M. Hennrich, and R. Blatt, Nat. Phys. **6**, 943 (2010).
[32] C. Weedbrook, S. Pirandola, R. García-Patrón, N. J. Cerf, T. C. Ralph, J. H. Shapiro, and S. Lloyd, Rev. Mod. Phys. **84**, 621 (2012).
[33] L. Cao, J. Qi, J. Du, and J. Jing, Phys. Rev. A **95**, 023803 (2017).
[34] S. Lv and J. Jing, Phys. Rev. A **96**, 043873 (2017).
[35] L. Cao, W. Wang, Y. Lou, J. Du, and J. Jing, Appl. Phys. Lett. **112**, 251102 (2018).
[36] V. Boyer, A. M. Marino, R. C. Pooser, and P. D. Lett, Science **321**, 544 (2008).
[37] A. M. Marino, R. C. Pooser, V. Boyer, and P. D. Lett, Nature (London) **457**, 859 (2009).
[38] P. van Loock and A. Furusawa, Phys. Rev. A **67**, 052315 (2003).
[39] A. Furusawa, J. L. Sørensen, S. L. Braunstein, C. A. Fuchs, H. J. Kimble, and E. S. Polzik, Science **282**, 706 (1998).
[40] L. M. Duan, G. Giedke, J. I. Cirac, and P. Zoller, Phys. Rev. Lett. **84**, 2722 (2000).
[41] R. Simon, Phys. Rev. Lett. **84**, 2726 (2000).